Entanglement and the interplay between staggered fields and couplings

Jenny Hide,[1,2] Yoshifumi Nakata,[2] and Mio Murao[2,3]
[1]*The Abdus Salam International Centre for Theoretical Physics, Strada Costiera 11, 34151 Trieste Italy*
[2]*Department of Physics, Graduate School of Science, University of Tokyo, Tokyo 113-0033, Japan*
[3]*Institute for Nano Quantum Information Electronics, University of Tokyo, Tokyo 153-8505, Japan*
(Received 19 January 2012; published 4 April 2012)

We investigate how the interplay between a staggered magnetic field and staggered coupling strength affects both ground-state and thermal entanglement. Upon analytically calculating thermodynamic quantities and the correlation functions for such a system, we consider both the global Meyer-Wallach measure of entanglement and the concurrence between pairs of spins. We discover two quantum critical points present in the model and show that the behavior of entanglement at zero temperature reflects each. We discover that increasing the alternating field and alternating coupling strength can actually increase the amount of entanglement present both at zero temperature and for thermal states of the system.

DOI: 10.1103/PhysRevA.85.042303 PACS number(s): 03.67.Bg, 03.65.Ud, 75.10.Jm

I. INTRODUCTION

Entanglement is an intriguing concept in quantum information, and a resource used in many quantum-computation schemes [1]. The Heisenberg coupling in spin chains has been shown to allow universal quantum computation [2]. Spin chains are also good candidates for quantum wires [3]. Thus it is an important task to explore how the amount of entanglement in such systems changes under different conditions, to discover whether it can be enhanced and what causes its destruction.

Many-body entanglement [1] is difficult to quantify, so entanglement measures are often restricted to the pure, zero-temperature case, for example, von Neumann entropy [4] or the Meyer-Wallach measure [5], or to a small number of possibly mixed qubits such as concurrence [6]. On the other hand, it is, in general, hard to quantitatively study entanglement of thermal states due to the absence of an efficient separability criterion for mixed states in many-body systems. An alternative approach is to use an entanglement witness which detects rather than measures entanglement. In particular, a thermodynamic entanglement witness uses thermodynamic quantities derived from the partition function of the system to detect entanglement [7,8].

In spin chains, ground-state entanglement is often investigated in the context of quantum phase transitions (QPTs). A QPT is a sudden change in the properties of the ground state when a parameter of the Hamiltonian such as a magnetic field is varied. Since it is expected that by investigation of QPTs, dramatic changes to physical quantities at very low temperature will be revealed, QPTs have been intensely studied in spin systems [9]. In Ref. [10], it was shown that, in general, a singularity occurs in the ground-state entanglement at quantum critical points (QCPs).

In this paper, we investigate entanglement of a spin system in a nonuniform magnetic field with nonuniform coupling constants. Certain solid-state systems such as copper benzoate have a nonuniform magnetic field [11], caused by an inhomogeneous Zeeman coupling. Similarly, examples exist for a nonuniform coupling strength [12,13]. Some properties of these materials can be captured using the staggered spin chain we study in this paper.

Entanglement in a staggered magnetic field has been studied previously using single-site entropy and an entanglement witness [14]. The effect of such a staggered field on the dynamics and on the high-fidelity transfer of entanglement has also been considered [15]; it was found that the staggered field is almost as efficient as the uniform case. On the other hand, entanglement in a spin chain with staggered coupling and magnetic field has been considered only for nearest neighbors in chains of finite length [16].

Here, we show how to calculate two measures of entanglement analytically for such spin chains with infinite length. We first calculate thermodynamic properties and finite-temperature correlation functions of the spin chain. Using these results, we show that the system exhibits QPTs at zero temperature induced by the staggered fields. We investigate global entanglement of the ground state using the Meyer-Wallach measure, a measure of multipartite pure states based on bipartite entanglement. We then investigate both zero- and finite-temperature entanglement between two spins using the concurrence. At zero temperature, we calculate the derivative of the concurrence and find that it diverges at the QCPs, and demonstrate that the global Meyer-Wallach measure is neither zero nor maximum at the QCPs, but changes to a constant value instead. Regarding the amount of entanglement, we find that global entanglement of the ground state in general increases with an alternating coupling constant. At zero temperature, the concurrence first increases, reaches a maximum, and then decreases with an alternating coupling constant. We also find that for certain values of magnetic field both the Meyer-Wallach measure and the zero-temperature concurrence can be increased by an alternating magnetic field. At finite temperature, the concurrence can again be increased by certain values of the staggered fields and couplings. Further, we examine entanglement at finite temperature using an entanglement witness with the aim of searching for thermal multipartite entanglement.

This paper is organized as follows. In Sec. II, we present the Hamiltonian and give its diagonal form, which allows us to calculate thermodynamical quantities of the system. We compute the correlation functions in Sec. III. In Sec. IV, we investigate the ground state and show that the Hamiltonian

exhibits QPTs. Then we investigate entanglement at zero temperature and at finite temperature in Sec. V. We present concluding remarks in Sec. VI.

II. THE HAMILTONIAN AND ITS THERMODYNAMIC PROPERTIES

We consider the thermodynamic limit of the staggered Hamiltonian

$$H = -\sum_{l=1}^{N}\left[\frac{J_l}{2}\left(\sigma_l^x\sigma_{l+1}^x + \sigma_l^y\sigma_{l+1}^y\right) + B_l\sigma_l^z\right], \tag{1}$$

where $J_l = J + e^{i\pi l}j$ is the staggered coupling strength and $B_l = B + e^{i\pi l}b$ is the staggered magnetic field. We refer to j as the alternating coupling strength and b as the alternating magnetic field. This spin chain can be diagonalized [17] using a Jordan-Wigner transformation $a_l = \prod_{m=1}^{l-1}\sigma_m^z \otimes (\sigma_l^x + i\sigma_l^y)/2$, with anticommutation relations $\{a_l,a_m\} = 0$ and $\{a_l^\dagger,a_m\} = \delta_{l,m}$, followed by a Fourier transform $a_l = N^{-1/2}\sum_k d_k e^{2i\pi kl/N}$. Next the Hamiltonian must be rewritten as a sum to $N/2$:

$$\begin{aligned} H = \sum_{k=1}^{N/2}&(\mu_k^- d_k^\dagger d_k + \mu_k^+ d_{k+N/2}^\dagger d_{k+N/2} \\ &+ \nu_k^+ d_k^\dagger d_{k+N/2} + \nu_k^- d_{k+N/2}^\dagger d_k - 2B\mathbf{1}) \end{aligned} \tag{2}$$

where $\mu_k^\pm = [2B \pm 2J\cos(2\pi k/N)]$ and $\nu_k^\pm = [2b \pm 2ij\sin(2\pi k/N)]$. This can now be diagonalized using a canonical transformation,

$$\begin{aligned} d_k &= \alpha_k\cos\theta_k + \beta_k\sin\theta_k, \\ d_{k+N/2} &= -\alpha_k\sin\theta_k + \beta_k\cos\theta_k, \end{aligned} \tag{3}$$

where θ_k is determined by $-J\cos(2\pi k/N)\sin 2\theta_k + b\cos 2\theta_k = ij\sin(2\pi k/N)$. Thus the diagonal form of the Hamiltonian is

$$H = \sum_{k=1}^{N/2}(\lambda_k^+\alpha_k^\dagger\alpha_k + \lambda_k^-\beta_k^\dagger\beta_k - 2B\mathbf{1}), \tag{4}$$

where $\lambda_k^\pm = 2B \pm 2\sqrt{J^2\cos^2(\frac{2\pi k}{N}) + b^2 + j^2\sin^2(\frac{2\pi k}{N})}$. The anticommutation relations are now $\{\alpha_l^\dagger,\alpha_m\} = \{\beta_l^\dagger,\beta_m\} = \delta_{l,m}$ and $\{\alpha_l,\alpha_m\} = \{\beta_l,\beta_m\} = \{\alpha_l^\dagger,\beta_m\} = \{\alpha_l,\beta_m\} = 0$. In all figures in the paper, we will fix J to 1 and use natural units.

The partition function $Z = \mathrm{tr}(e^{-\beta H})$ of this system can be written $Z = \prod_{k=1}^{N/2} Z_k$ and thus $\ln Z = \sum_{k=1}^{N/2}\ln Z_k$, where $Z_k = [e^{2\beta B} + e^{-\beta(\lambda_k^- - 2B)} + e^{-\beta(\lambda_k^+ - 2B)} + e^{-2\beta B}]$ is found from the kth term in the Hamiltonian sum. Explicitly taking the thermodynamic limit, we find

$$\ln Z = \frac{N}{2\pi}\int_0^\pi dq\,\ln[4\cosh(\beta\Lambda_q^+)\cosh(\beta\Lambda_q^-)], \tag{5}$$

where $\Lambda_q^\pm = B \pm \sqrt{J^2\cos^2 q + b^2 + j^2\sin^2 q}$. From this, other thermodynamic quantities such as the internal energy $U = -\frac{\partial}{\partial\beta}\ln Z$ can be calculated:

$$u := \frac{U}{N} = -\int_0^\pi \frac{dq}{2\pi}[\Lambda_q^+\tanh(\beta\Lambda_q^+) + \Lambda_q^-\tanh(\beta\Lambda_q^-)]. \tag{6}$$

The magnetization $M = \frac{1}{\beta}\frac{\partial}{\partial B}\ln Z$ is

$$m := \frac{M}{N} = \int_0^\pi \frac{dq}{2\pi}[\tanh(\beta\Lambda_q^+) + \tanh(\beta\Lambda_q^-)], \tag{7}$$

and the staggered magnetization $M_s = \frac{1}{\beta}\frac{\partial}{\partial b}\ln Z$ is

$$m_s := \frac{M_s}{N} = \int_0^\pi \frac{dq}{2\pi}\frac{b[\tanh(\beta\Lambda_q^+) - \tanh(\beta\Lambda_q^-)]}{\sqrt{J^2\cos^2 q + b^2 + j^2\sin^2 q}}. \tag{8}$$

III. CORRELATION FUNCTIONS

We will use the correlation functions of the system to calculate each measure of entanglement. Since $[H, \sum_l \sigma_l^z] = 0$, the only nonzero correlation functions of this spin chain are $\langle\sigma_l^x\sigma_{l+R}^x + \sigma_l^y\sigma_{l+R}^y\rangle$, $\langle\sigma_l^z\sigma_{l+R}^z\rangle$, and $\langle\sigma_l^z\rangle$. The Hamiltonian is semi-translationally-invariant in that all odd and all even sites can be considered identical in the thermodynamic limit. Due to this semi-translational-invariance, when R is even, $\langle\sigma_l^z\rangle = \langle\sigma_{l+R}^z\rangle$.

We calculate each of the correlation functions following the method in Ref. [18]. We find these for any R. Generally, $\langle\sigma_l^x\sigma_{l+R}^x + \sigma_l^y\sigma_{l+R}^y\rangle = 2\langle a_l^\dagger\prod_{m=l+1}^{R-1}(\mathbf{1} - 2a_m^\dagger a_m)a_{l+R} + a_{l+R}^\dagger\prod_{m=l+1}^{R-1}(\mathbf{1} - 2a_m^\dagger a_m)a_l\rangle$, $\langle\sigma_l^z\sigma_{l+R}^z\rangle = \langle(\mathbf{1} - 2a_l^\dagger a_l)(\mathbf{1} - 2a_{l+R}^\dagger a_{l+R})\rangle$, and $\langle\sigma_l^z\rangle = \langle\mathbf{1} - 2a_l^\dagger a_l\rangle$.

The autocorrelation functions of this model have been found analytically in the infinite-temperature limit [19], and the time-dependent $\langle\sigma_l^z(t)\sigma_{l+R}^z\rangle$ has been found, also analytically, for arbitrary temperature [20]. However, the general equilibrium correlation functions have not been calculated previously to our knowledge.

Since the spin chain is a free-fermion model and semi-translationally-invariant, Wick's theorem can be applied to the total correlation functions. Thus we can rewrite each of the above equations in terms of two-point correlation functions. For example, the zz correlation function is $\langle(\mathbf{1} - 2a_l^\dagger a_l)(\mathbf{1} - 2a_{l+R}^\dagger a_{l+R})\rangle = \langle\sigma_l^z\rangle\langle\sigma_{l+R}^z\rangle - G_{l,R}^2$, where we have defined $G_{l,R} = -\langle a_l^\dagger a_{l+R} - a_l a_{l+R}^\dagger\rangle$. We use the notation $G_{l,R} = G_R^0 + e^{i\pi l}G_R^s$ and $\langle\sigma_l^z\rangle = \langle\sigma^z\rangle^0 + e^{i\pi l}\langle\sigma^z\rangle^s$ where $G_R^0 = -\frac{1}{N}\sum_l\langle a_l^\dagger a_{l+R} - a_l a_{l+R}^\dagger\rangle$ and $G_R^s = -\frac{1}{N}\sum_l e^{i\pi l}\langle a_l^\dagger a_{l+R} - a_l a_{l+R}^\dagger\rangle$ (similarly for $\langle\sigma_l^z\rangle$). Note that we have treated $\langle\sigma_l^z\rangle$ separately from $G_{l,R}$ despite the fact that $R = 0$ should give us $\langle\sigma_l^z\rangle$. The reason for this will become clear below.

Using the Jordan-Wigner transformation and Fourier transform and then summing to $N/2$ (the additional canonical transformation is unnecessary), we find we can write

$$\begin{aligned} \langle\sigma_l^z\rangle^0 &= \frac{1}{N}\sum_{k=1}^{N/2}[\langle\mathbf{1} - 2d_k^\dagger d_k\rangle + \langle\mathbf{1} - 2d_{k+N/2}^\dagger d_{k+N/2}\rangle], \\ \langle\sigma_l^z\rangle^s &= -\frac{2}{N}\sum_{k=1}^{N/2}[\langle d_k^\dagger d_{k+N/2}\rangle + \langle d_{k+N/2}^\dagger d_k\rangle], \end{aligned} \tag{9}$$

for $\langle\sigma_l^z\rangle$ and

$$G_R^0 = \frac{1}{N}\sum_{k=1}^{N/2}\cos\left(\frac{2\pi kR}{N}\right)[\langle \mathbf{1} - 2d_k^\dagger d_k\rangle + e^{i\pi R}\langle \mathbf{1} - 2d_{k+N/2}^\dagger d_{k+N/2}\rangle],$$
$$G_R^s = \frac{2i}{N}\sum_{k=1}^{N/2}\sin\left(\frac{2\pi kR}{N}\right)[\langle d_k^\dagger d_{k+N/2}\rangle + e^{i\pi R}\langle d_{k+N/2}^\dagger d_k\rangle], \tag{10}$$

for $G_{l,R}$. We know the thermodynamic forms of $\langle\sigma_l^z\rangle^0 = m$ [Eq. (7)] and $\langle\sigma_l^z\rangle^s = m_s$ [Eq. (8)], and also of $G_{l,1} = -\langle\sigma_l^x\sigma_{l+1}^x + \sigma_l^y\sigma_{l+1}^y\rangle/2$, which can be calculated by differentiating the partition function with respect to the coupling strengths, $G_{l,1}^0 = -\frac{1}{N\beta}\frac{\partial}{\partial J}\ln Z$ and $G_{l,1}^s = -\frac{1}{N\beta}\frac{\partial}{\partial j}\ln Z$. Thus we have

$$G_1^0 = -\int_0^\pi \frac{dq}{2\pi}\frac{J\cos^2 q[\tanh(\beta\Lambda^+) - \tanh(\beta\Lambda^-)]}{\sqrt{J^2\cos^2 q + b^2 + j^2\sin^2 q}},$$
$$G_1^s = -\int_0^\pi \frac{dq}{2\pi}\frac{j\sin^2 q[\tanh(\beta\Lambda^+) - \tanh(\beta\Lambda^-)]}{\sqrt{J^2\cos^2 q + b^2 + j^2\sin^2 q}}.$$

The thermodynamic expressions for $G_{l,R}$ are found directly from the above equations. For even R, we compare the correlation function form of $G_{l,R}$ to that of $\langle\sigma_l^z\rangle$, noticing that they are similar. Since we know the thermodynamic form of $\langle\sigma_l^z\rangle$, we can also determine the thermodynamic form of $G_{l,R}$:

$$G_R^0 = \int_0^\pi \frac{dq}{2\pi}\cos(qR)[\tanh(\beta\Lambda^+) + \tanh(\beta\Lambda^-)],$$
$$G_R^s = -i\int_0^\pi \frac{dq}{2\pi}\frac{b\sin(qR)[\tanh(\beta\Lambda^+) - \tanh(\beta\Lambda^-)]}{\sqrt{J^2\cos^2 q + b^2 + j^2\sin^2 q}}. \tag{11}$$

We note that for R even, $G_R^s = 0$. For odd R, we instead compare the correlation function form of $G_{l,R}$ to $G_{l,1}$, again noticing they are similar. Using the thermodynamic form of $G_{l,1}$, we determine the thermodynamic form of $G_{l,R}$:

$$G_R^0 = -\int_0^\pi \frac{dq}{2\pi}\cos(qR)\frac{J\cos q[\tanh(\beta\Lambda^+) - \tanh(\beta\Lambda^-)]}{\sqrt{J^2\cos^2 q + b^2 + j^2\sin^2 q}},$$
$$G_R^s = -\int_0^\pi \frac{dq}{2\pi}\sin(qR)\frac{j\sin q[\tanh(\beta\Lambda^+) - \tanh(\beta\Lambda^-)]}{\sqrt{J^2\cos^2 q + b^2 + j^2\sin^2 q}}.$$

The differences between odd and even R are due to the presence of the $e^{i\pi R}$ term in the correlation-function forms of $G_{l,R}$.

IV. PROPERTIES OF THE GROUND STATE

In this section, we investigate the properties of the ground state. Without the alternating coupling strength and the alternating magnetic field, the Hamiltonian is referred to as an XX model with a transverse magnetic field. It is well known that the XX model has a second-order QPT at $B = J$ [21]. We investigate the ground-state energy as a function of the alternating coupling strength and the alternating magnetic field, and see the QPTs induced by them.

We first define Q as

$$Q = \{Q \in [0,\pi]|\Lambda_q^- < 0\}. \tag{12}$$

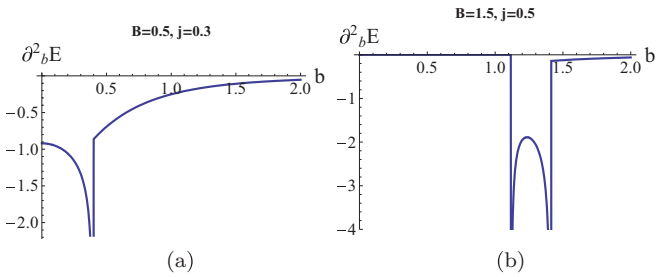

FIG. 1. (Color online) Second derivative of the ground-state energy with respect to b. (a) and (b) are for $(B,j) = (0.5,0.3)$ and $(B,j) = (1.5,0.5)$, respectively. It is observed that the second derivative diverges at the QCPs $B = \sqrt{J^2 + b^2}$ and $B = \sqrt{j^2 + b^2}$.

For simplicity, we also introduce two functions,

$$\Theta(q) = \sqrt{J^2\cos^2 q + b^2 + j^2\sin^2 q}, \tag{13}$$

$$\Xi = \arccos\sqrt{\frac{B^2 - b^2 - j^2}{J^2 - j^2}}. \tag{14}$$

By using the internal energy per site u given by Eq. (6), the ground-state energy per site is obtained by taking a limit such as

$$\epsilon_g = -\lim_{\beta\to\infty}\int_0^\pi \frac{dq}{2\pi}[\Lambda_q^+\tanh(\beta\Lambda_q^+) + \Lambda_q^-\tanh(\beta\Lambda_q^-)]$$
$$= -\int_{q\notin Q}\frac{dq}{2\pi}[\Lambda_q^+ + \Lambda_q^-] - \int_{q\in Q}\frac{dq}{2\pi}[\Lambda_q^+ - \Lambda_q^-]$$
$$= -B + \frac{1}{\pi}\int_{q\in Q}[B - \Theta(q)]dq. \tag{15}$$

In the Appendix, the region Q is analytically obtained and exact expressions of the ground-state energy are shown. In order to visualize the QPTs, the second derivative of the ground state in terms of b for $(B,j) = (0.5,0.3)$ and $(B,j) = (1.5,0.5)$ is given in Fig. 1. It is observed that the derivative diverges at the points $B = \sqrt{J^2 + b^2}$ and $B = \sqrt{j^2 + b^2}$, both of which lead to second-order QPTs.

The QPTs are observed more clearly by looking at the magnetic susceptibility at zero temperature. In the Appendix, the magnetization at zero temperature is explicitly calculated; it is a function of Ξ. Since the derivative of Ξ with respect to B and b includes a factor $1/\sqrt{B^2 - b^2 - j^2}\sqrt{-B^2 + J^2 + b^2}$, the derivative diverges at the points $B = \sqrt{J^2 + b^2}$ and $B = \sqrt{j^2 + b^2}$, which implies QPTs. To demonstrate this, we also plot the magnetization at zero temperature in Fig. 2. We can clearly see that the magnetization of the ground state changes nonsmoothly at both QCPs.

We note that, when $j = b = 0$ corresponding to the XX model with a transverse magnetic field, $B = \sqrt{J^2 + b^2}$ reduces to the QCP of the XX model, $B = J$. On the other hand, QPTs at $B = \sqrt{j^2 + b^2}$ do not appear in the XX model. Hence this QCP can be regarded as being induced by the staggered nature of the spin chain.

V. ENTANGLEMENT

We study entanglement properties of the spin chain in three different ways. First we define the Meyer-Wallach

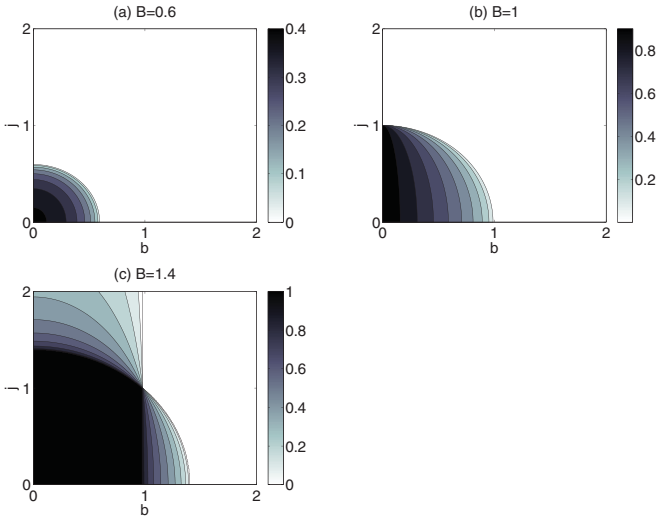

FIG. 2. (Color online) Magnetization at zero temperature. (a), (b), and (c) show $B = 0.6$, 1, and 1.4, respectively. The magnetization changes nonsmoothly at the quantum critical points $B = \sqrt{J^2 + b^2}$ and $B = \sqrt{j^2 + b^2}$.

measure and the concurrence and discuss how to calculate each for the staggered Hamiltonian. Next we consider how both entanglement measures behave at zero temperature, and then how a finite temperature affects the concurrence. Finally we consider a thermodynamic entanglement witness in an attempt to detect thermal entanglement which the measures miss, such as multipartite entanglement. In case of degeneracy in the ground state, the description of the ground state depends on how the degeneracy is dealt with, as does the amount of entanglement of the ground state. In this paper, we calculate entanglement of the ground state obtained by taking the zero-temperature limit of thermal states in the thermodynamic limit.

A. Meyer-Wallach measure and concurrence

First, we show how to calculate the Meyer-Wallach measure and the concurrence from the thermodynamic quantities calculated in Sec. II and correlation functions in Sec. III. For a pure state $|\Phi\rangle$ of an N-spin system, the Meyer-Wallach measure is defined by

$$E_{\mathrm{MW}}(|\Phi\rangle) = 2 - \frac{2}{N}\sum_{i=1}^{N} \mathrm{Tr}\rho_i^2,$$

where $\rho_i := \mathrm{Tr}_{\neg i}|\Phi\rangle\langle\Phi|$ is the reduced density matrix at the ith spin [5,22]. (The partial trace $\mathrm{Tr}_{\neg i}$ is taken over all degrees of freedom except the ith spin.) The Meyer-Wallach measure takes values between 0 and 1. The minimum is achieved if and only if the state is separable, while the maximum is given by states which are local unitary equivalents to the Greenberger-Horne-Zeilinger (GHZ) state. The Meyer-Wallach measure is a measure of *global* entanglement [5], namely, it reflects the properties of entanglement in the total N-spin states. It is investigated in the context of QPTs where the Meyer-Wallach measure is shown to behave nonanalytically at QCPs [23–25].

We calculate the entanglement of the ground state found by the Meyer-Wallach measure. Since the Hamiltonian preserves the magnetization, i.e., $[H, \sum_l \sigma_l^z] = 0$, the reduced density matrix of a spin at site l, ρ_l, has only diagonal elements such that $\rho_l = \mathrm{diag}\{\frac{1+\langle\sigma_l^z\rangle_g}{2}, \frac{1-\langle\sigma_l^z\rangle_g}{2}\}$, where $\langle\sigma_l^z\rangle_g := \langle g|\sigma_l^z|g\rangle$ is the expectation value of σ_l^z in the ground state $|g\rangle$. By substituting this and using the fact that the Hamiltonian is semi-translationally-invariant, we obtain the Meyer-Wallach measure of the ground state as

$$E_{\mathrm{MW}}(|g\rangle) = 1 - \tfrac{1}{2}\left(\left\langle\sigma_{\mathrm{even}}^z\right\rangle_g^2 + \left\langle\sigma_{\mathrm{odd}}^z\right\rangle_g^2\right), \tag{16}$$

where $\langle\sigma_{\mathrm{even}}^z\rangle_g = \langle g|\sigma_{2l}^z|g\rangle$ and $\langle\sigma_{\mathrm{odd}}^z\rangle_g = \langle g|\sigma_{2l+1}^z|g\rangle$ for any l. The $\langle\sigma_{\mathrm{even}}^z\rangle$ and $\langle\sigma_{\mathrm{odd}}^z\rangle$ are obtained from the magnetization m given by Eq. (7) and m_s given by Eq. (8), such that

$$\left\langle\sigma_{\mathrm{even}}^z\right\rangle_g = \lim_{\beta\to\infty}[m + m_s], \tag{17}$$

$$\left\langle\sigma_{\mathrm{odd}}^z\right\rangle_g = \lim_{\beta\to\infty}[m - m_s]. \tag{18}$$

The exact expressions of the ground-state energy, the magnetization at zero temperature, and the Meyer-Wallach measure are given in the Appendix. The Meyer-Wallach measure of the ground state behaves nonanalytically at QCPs, reflecting the fact that it is a function of the magnetization.

The concurrence $\mathcal{C}$ between two spins [6] is an entanglement measure for both pure and mixed states, and can therefore be used at finite temperatures. It is given by

$$\mathcal{C}(\rho) = \max\{0, \lambda_1 - \lambda_2 - \lambda_3 - \lambda_4\}, \tag{19}$$

where the λ_i's are the square roots of the eigenvalues of the matrix $\rho\tilde{\rho}$ with $\tilde{\rho} = (\sigma^y \otimes \sigma^y)\rho^*(\sigma^y \otimes \sigma^y)$, and satisfy $\lambda_1 \geqslant \lambda_2 \geqslant \lambda_3 \geqslant \lambda_4$. Again using $[H, \sum_l \sigma_l^z] = 0$, the concurrence between two spins at sites l and $l + R$ is $\mathcal{C}(\rho_{l,l+R}) = 2\max\{0, |z| - \sqrt{vy}\}$, where $z = \frac{1}{4}\langle\sigma_l^x\sigma_{l+R}^x + \sigma_l^y\sigma_{l+R}^y\rangle$, and $vy = \frac{1}{16}[(1 + \langle\sigma_l^z\sigma_{l+R}^z\rangle)^2 - (\langle\sigma_l^z\rangle + \langle\sigma_{l+R}^z\rangle)^2]$. Due to the semi-translational-invariance of the Hamiltonian, the concurrence is the same for all odd sites and for all even sites. The concurrence is zero if and only if the state of the two spins is separable and is 1 when they are maximally entangled. Although we could calculate the concurrence for any R, we concentrate on the nearest-neighbor, $\mathcal{C}_1$ with $R = 1$, and the next-nearest-neighbor, $\mathcal{C}_2$ with $R = 2$, concurrence, since for large R the concurrence is infinitesimal. Using $\langle\sigma_l^z\sigma_{l+R}^z\rangle = \langle\sigma_l^z\rangle\langle\sigma_{l+R}^z\rangle - G_{l,R}^2$, the nearest-neighbor concurrence is

$$\mathcal{C}_1 = \max\left\{0, |G_{l,1}| - \tfrac{1}{2}\sqrt{\left(1 + \left\langle\sigma_l^z\sigma_{l+1}^z\right\rangle\right)^2 - (2\langle\sigma^z\rangle^0)^2}\right\}, \tag{20}$$

and the next-nearest-neighbor concurrence is

$$\mathcal{C}_2 = \max\left\{0, \left|G_{l,1}G_{l+1,1} - G_{l,2}\left\langle\sigma_{l+1}^z\right\rangle\right| - \tfrac{1}{2}\sqrt{\left(1 + \left\langle\sigma_l^z\sigma_{l+2}^z\right\rangle\right)^2 - \left(2\left\langle\sigma_l^z\right\rangle\right)^2}\right\}, \tag{21}$$

remembering that $G_{l,R}$ is different for odd and for even values of R.

When $J = j$, the total coupling strength between nearest-neighbor sites for odd l is zero, while for even l, it is $2J$. Thus, at any temperature, there is no entanglement between nearest neighbors for odd sites, and at zero temperature (and magnetic fields), the chain consists of $N/2$ maximally entangled singlet states. This is an example of dimerization. As a consequence

of this, there is also no concurrence at $J = j$ for both odd and even sites for any $R > 1$.

In the following, we investigate entanglement in the ground state in terms of the Meyer-Wallach measure and the concurrence, as well as in the thermal state in terms of the concurrence. The Meyer-Wallach measure is a measure of global entanglement of the total N-spin state, whereas the concurrence is a measure of entanglement of a reduced two-spin density matrix. When the Meyer-Wallach measure is zero, the concurrence between any two spins is also zero. However, a large amount of the Meyer-Wallach measure does not necessarily imply a large amount of concurrence between two spins. For instance, the Meyer-Wallach measure is 1 but the concurrence between any two spins is zero for the GHZ state. By calculating both of them, we study multilateral properties of entanglement contained in the ground state. It should be noted that the Meyer-Wallach measure is a measure of entanglement only for a pure state and thus is meaningful for investigation of entanglement in the ground state but not that of thermal states, in contrast to the concurrence.

B. Zero temperature

In this section, we study entanglement at zero temperature using the Meyer-Wallach measure and the concurrence as defined above. Figures 3 and 4 show the Meyer-Wallach measure, Figs. 5 and 6 the nearest-neighbor (NN) concurrence for both odd and even sites, and Fig. 7 the next-nearest-neighbor (NNN) concurrence.

1. Quantum phase transitions

We first discuss the Meyer-Wallach measure of the ground state. See the Appendix for the detailed calculation. In Figs. 3 and 4, it is observed that the Meyer-Wallach measure changes nonsmoothly at the QCPs.

Conversely, considering the plots for concurrence at zero temperature, the quantum phase transitions present in the staggered model are not always evident. In particular, when B is plotted against b for odd sites in Fig. 5, only the

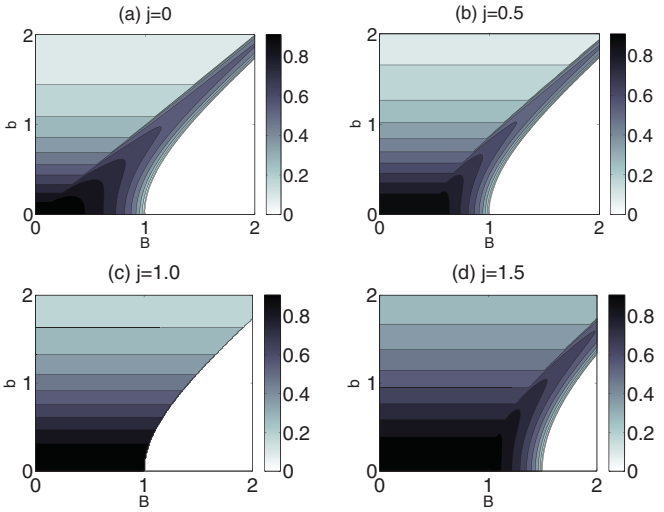

FIG. 3. (Color online) The Meyer-Wallach measure as a function of B and b.

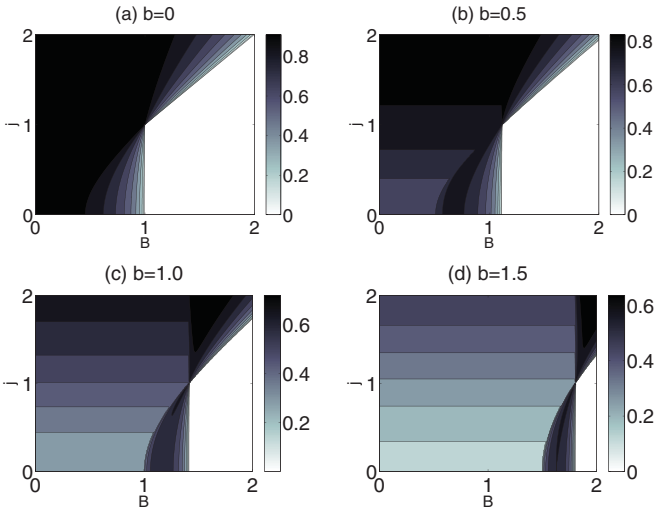

FIG. 4. (Color online) The Meyer-Wallach measure as a function of B and j.

curve $B = \sqrt{J^2 + b^2}$ can be seen in Fig. 5(b), while only $B = \sqrt{j^2 + b^2}$ can be seen in Fig. 5(c). However, changes in the concurrence can be observed at both QCPs for even l in the same figure, and for both odd and even sites in Fig. 6 where we plot B against j. These results are consistent with the results in Ref. [10], where it is shown that entanglement of the ground state behaves singularly around QCPs in general.

In order to probe the quantum phase transition further, we plot both the derivative of the concurrence (for $T \to 0$) with respect to $\alpha = 1/B$ and the Meyer-Wallach measure as

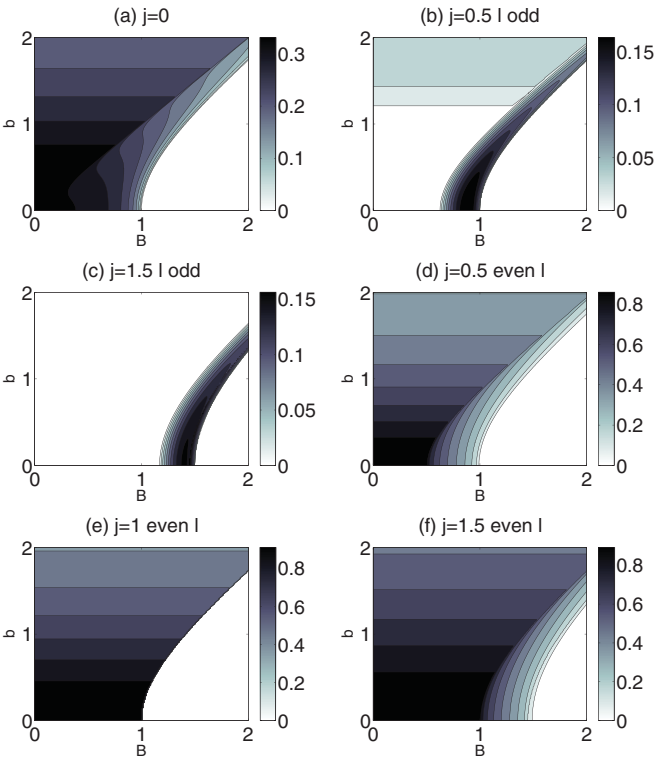

FIG. 5. (Color online) The nearest-neighbor concurrence as a function of B and b as $T \to 0$.

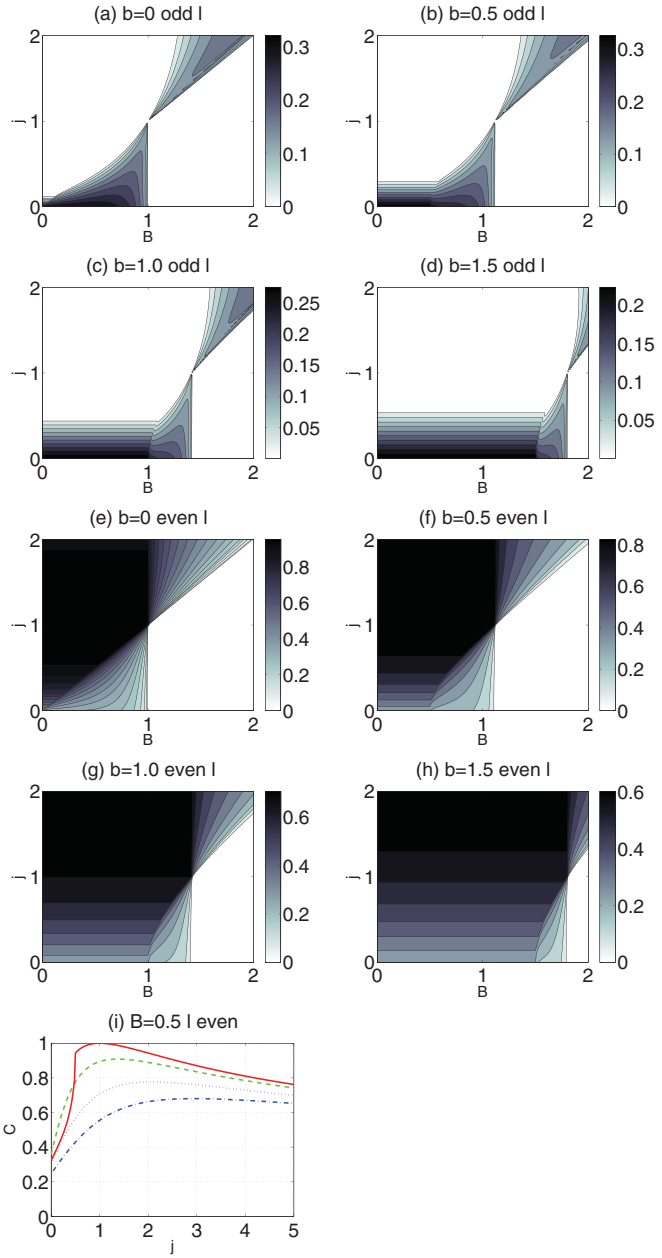

FIG. 6. (Color online) The nearest-neighbor concurrence as a function of B and j as $T \to 0$. (i) plots the concurrence against j for l even, $B = 0.5$ to show that the concurrence decreases for high enough j for $b = 0$ (solid red line), 0.5 (dashed green line), 1 (dotted purple line), and 1.5 (dot-dashed blue line).

a function of α (Fig. 8) as was done for the XY spin chain in Ref. [26]. It has been reported in some spin models that, on taking an appropriate superposition of degenerate ground states, global measures such as the Meyer-Wallach measure display either a maximum or a change to zero entanglement at the QCP, while derivatives of the bipartite entanglement measures such as concurrence diverge at the critical point [23,24,27–29]. Such behavior of global entanglement at the QCPs in the staggered model is not observed in Fig. 8; while the derivative of the concurrence with respect to α indeed exhibits divergences at both critical points, the Meyer-Wallach measure is neither zero nor maximum at some critical points.

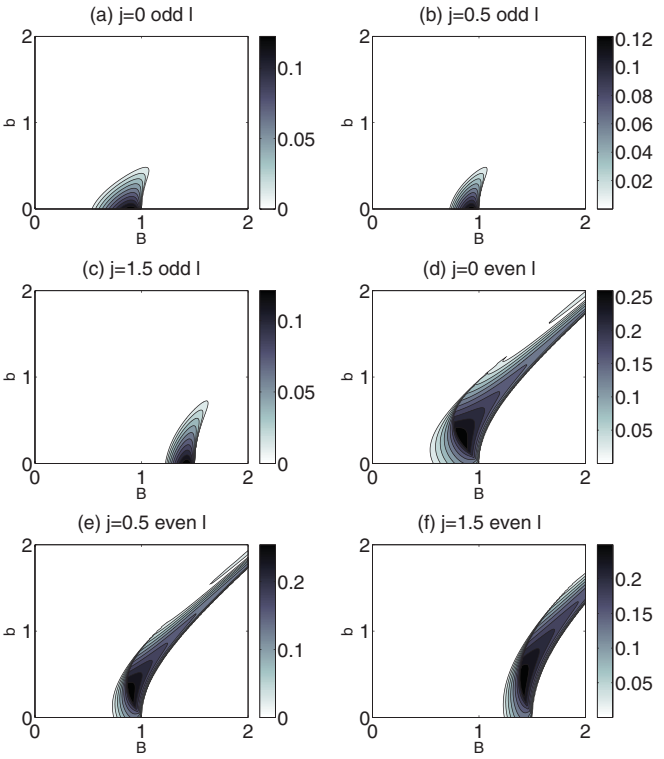

FIG. 7. (Color online) Next-nearest-neighbor concurrence as $T \to 0$. Concurrence is zero when $j = 1$ as discussed in the text.

Moreover, in our case, the magnetization of the ground state in the thermodynamic limit does not change on taking different superpositions of degenerate ground states, and therefore neither does the Meyer-Wallach measure, which is a function of the magnetization. Hence, global entanglement of the ground state for the staggered Hamiltonians cannot show a maximum or a change to zero entanglement at the QCP. The invariance of the Meyer-Wallach measure under superpositions in our

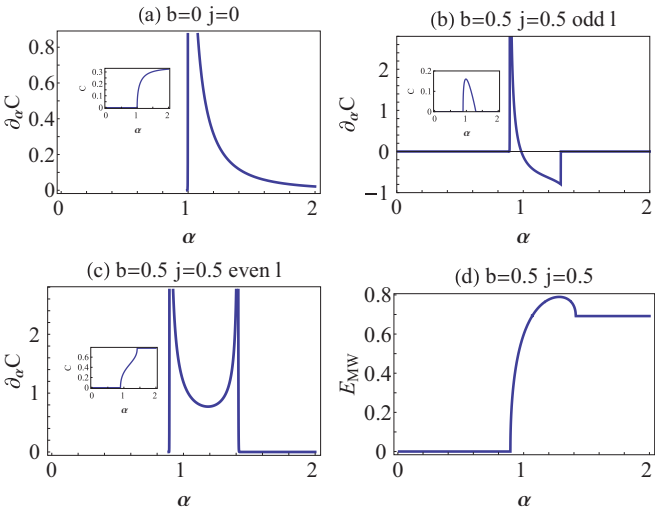

FIG. 8. (Color online) (a), (b), and (c) show the derivative of the concurrence with respect to $\alpha = 1/B$. In each, the inset shows the behavior of the concurrence itself as a function of α. (d) plots the Meyer-Wallach measure against α.

models justifies the use of the Meyer-Wallach measure to quantify global entanglement of the ground state for staggered Hamiltonian systems.

Finally, related to the phase diagram of the *XX* model, we make a remark on our figures concerning the ambiguity of the amount of entanglement for the degenerate ground state in finite systems. When $j = b = 0$, the Hamiltonian reduces to the *XX* model. By taking a superposition of degenerate ground states at $B = 1$, we can choose a separable ground state without taking the thermodynamic limit [30], whereas if we take a mixture of two degenerate states, the resulting state is still weakly entangled [31]. The choice of the separable ground state is observed in our figures, that is, both of the Meyer-Wallach measure and the concurrence are zero at $B = 1$ when $j = b = 0$. In other parameter regions where entanglement is zero, the ground state is separable only in the thermodynamic limit.

2. *Effects of j and b on entanglement*

Next, we discuss the effects of b and j on the Meyer-Wallach measure and the concurrence. First, we consider the effect of b on entanglement, shown in Figs. 3 and 5. How the concurrence behaves in the presence of alternating fields is highly dependent on whether the site is odd or even. In general, due to the larger coupling from an even site to an odd site, both nearest- and next-nearest-neighbor concurrence are higher, with the opposite being true from an odd to an even site. Entanglement for the Meyer-Wallach measure and odd-site NN concurrence remains large only when B is between the two QPTs, i.e., $\sqrt{j^2+b^2} < B < \sqrt{J^2+b^2}$ when $j < J$ or $\sqrt{J^2+b^2} < B < \sqrt{j^2+b^2}$ when $J < j$. For both measures, the maximum entanglement is at $B \sim b$ for large magnetic fields. These results are understandable from the fact that a large magnetic field aligns spins in the same direction, leading to a separable state. When b and B are large, entanglement can be large only for $B \sim b$, since the magnetic field on odd sites is canceled in such cases. The even-site NN concurrence does not follow this pattern, and instead a larger amount of entanglement tends to be present when $B < \sqrt{j^2+b^2}$ for $j < J$ or when $B < \sqrt{J^2+b^2}$ for $J < j$.

On the other hand, the Meyer-Wallach measure and the concurrence vary differently with the alternating coupling constant j as shown in Figs. 4 and 6, where entanglement is plotted as a function of j. The Meyer-Wallach measure is an increasing function with j except in the vicinity of the QCPs while the concurrence is in general a decreasing function of j. Figure 6(i) shows that for each b there is a nonzero value of j for which the concurrence is the maximum possible. Since the Meyer-Wallach measure is a measure of entanglement shared in the whole spin chain and the concurrence measures entanglement between two spins, we can conclude from these results that, as the alternating coupling constant j increases, the amount of entanglement shared among all spins increases. Such global entanglement is not locally detected, in the sense that entanglement of the reduced two-spin state is small.

The concurrence is closely related to entanglement of formation. In Fig. 6, for odd sites, when $B > \sqrt{J^2+b^2}$, increasing j can increase concurrence, and for even sites, when $B < \sqrt{j^2+b^2}$, increasing j increases the concurrence until a maximal value is reached, after which the concurrence decreases again. Thus a low but nonzero value of j can be beneficial to the extraction of the maximally entangled state.

Another interesting feature common to both the Meyer-Wallach measure and the concurrence, demonstrated in Figs. 3–6, is that below the region of the QCPs, entanglement is constant as B varies. That is, the magnetic field B is not a dominant parameter for entanglement below the QCPs. The QPTs are often intuitively understood as occurring due to the balance between the strength of the coupling constants and that of the magnetic fields. As such, the dominant parameters of this system are the coupling constants (the magnetic fields) below (above) the QCPs in general. Our results support this intuition from the viewpoint of entanglement in the sense that the magnetic field B does not change entanglement below the QCPs. On the other hand, entanglement is sensitive to the change of the alternating magnetic field b even below the QCPs, which demonstrates the difference between B and b.

Finally, the NNN concurrence is reduced compared to NN concurrence as expected, but remains reasonably high, especially for even sites where a nonzero value of b increases the entanglement. Further, increasing b allows a spin chain with larger values of B to be entangled.

We have also calculated third-nearest-neighbor concurrence with $R = 3$, but do not give the figures here. We observe similar plots to Fig. 7, but with the features for odd and even sites reversed such that similar regions (but with less entanglement) to those in Figs. 7(d), 7(e), and 7(f) is seen for odd rather than even sites. This follows from the staggered nature of the chain.

C. Finite temperature

We next investigate entanglement properties of the thermal states of the Hamiltonian using the concurrence. Figure 9 shows the nearest-neighbor concurrence for both odd and even sites for varying temperature and alternating coupling strength j. The figures show that increasing j allows the spin chain to be entangled at higher temperatures, and that increasing both b and B can enlarge the region of entanglement. That is, the spin chain is entangled for more values of T and j for higher b and B. This is true for even as well as odd sites. Next-nearest-neighbor concurrence can be seen in Fig. 10, where we again see that increasing the magnetic fields can be beneficial to entanglement. The third-nearest-neighbor concurrence is nonzero only for the parameter values studied (i.e., those in Fig. 9) when $b = 0$ and $B = 5$. The plots (not shown) for odd and even sites are similar to Fig. 10(a), but the amount of entanglement is less and odd-site and even-site concurrences are no longer identical. As discussed previously, there is no entanglement at $j = 1$ for odd sites at any temperature.

Increasing temperature has the effect of mixing energy levels, something which has the ability to either increase or decrease entanglement, although a high enough temperature will destroy entanglement. Increasing the alternating coupling strength counteracts this to some extent, although a high enough temperature still destroys the concurrence.

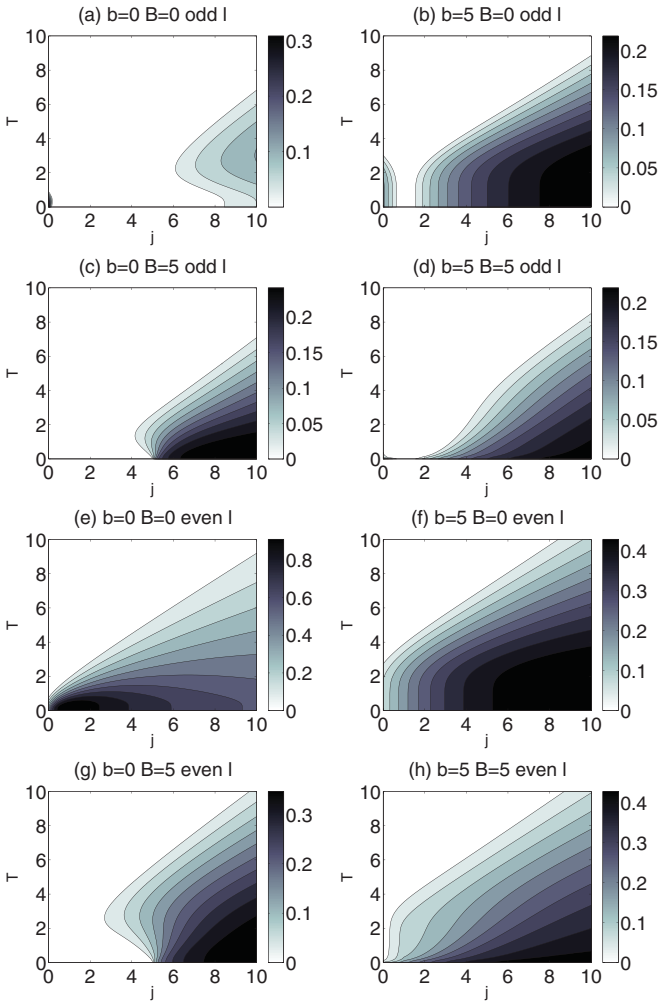

FIG. 9. (Color online) Nearest-neighbor concurrence for odd and even sites.

We note that increasing b allows larger values of concurrence at higher temperatures at lower, more accessible values of j as demonstrated in Figs. 9(b) and 9(f). Thus, here, it is the combination of alternating fields b and j that allows the spin chain to be entangled at higher temperatures. Increasing B has a similar effect, although to a lesser extent.

D. An entanglement witness

In order to detect rather than measure entanglement in this system, we use an entanglement witness based on the

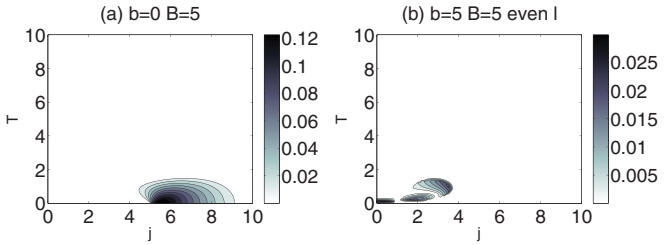

FIG. 10. (Color online) Next-nearest-neighbor concurrence. When $b = 0$ and $B = 5$, (a), the plot for odd and even sites is identical. No next-nearest-neighbor concurrence is found for the other values of B and b shown for nearest-neighbor concurrence.

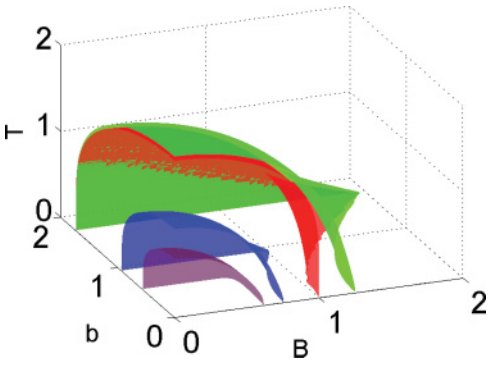

FIG. 11. (Color online) We witness entanglement at different values of the alternating coupling strength j for $j = 0$ (purple), 0.5 (blue), 1 (red), and 1.5 (green), from inside to out.

expectation value of the Hamiltonian:

$$\frac{4|U + BM + bM_s|}{N(|J - j| + |J + j|)} \leqslant 1, \tag{22}$$

where U is the internal energy [Eq. (6)], M is the magnetization [Eq. (7)], and M_s is the staggered magnetization [Eq. (8)]. The bound is found similarly to the usual method [7,8]. Rearrangement of the expectation value of the Hamiltonian gives $2|U + BM + bM_s| = |J \sum_l \langle \sigma_l^x \sigma_{l+1}^x + \sigma_l^y \sigma_{l+1}^y \rangle + j \sum_l e^{i\pi l} \langle \sigma_l^x \sigma_{l+1}^x + \sigma_l^y \sigma_{l+1}^y \rangle|$. The absolute value allows us to write $4|U + BM + bM_s|/N \leqslant |(J - j)||\langle \sigma_l^x \sigma_{l+1}^x + \sigma_l^y \sigma_{l+1}^y \rangle|_{l,\text{odd}} + |J + j||\langle \sigma_l^x \sigma_{l+1}^x + \sigma_l^y \sigma_{l+1}^y \rangle|_{l,\text{even}}$. Next, the bound for both the odd and even l for pure product states can be found using the Cauchy-Schwarz inequality and the definition of the density matrix, giving $|\langle \sigma_l^x \sigma_{l+1}^x + \sigma_l^y \sigma_{l+1}^y \rangle| \leqslant 1$. Due to the convexity of the set of separable states, this bound is also true for all separable states, while an entangled state can violate this bound.

Figure 11 demonstrates that an increase in the alternating coupling strength increases the region of entanglement detected by the witness. That is, at larger j, entanglement is detected for higher values of B, b, and T than is possible at smaller j. This trend persists even at very high values of j. In addition, the alternating magnetic field increases the maximum values of B for which entanglement is detected. However, overall, a sufficient increase in B, b, or T (except at $B \sim b$ as discussed in Sec. V B) will destroy entanglement either by causing the spins to align with the magnetic field, or via the mixing of energy levels as the temperature is raised.

The entanglement witness generally complements the results of the entanglement measures and allows for the possibility of detecting multipartite entanglement that cannot be measured by them. However, for our Hamiltonian, a comparison of Fig. 11 to Figs. 9 and 10 shows that this witness does not detect any extra entangled regions compared to the concurrence.

VI. CONCLUDING REMARKS

We have found that the introduction of an alternating coupling strength and alternating magnetic field into the usual XX spin chain in a uniform magnetic field can, for

certain values of the parameters, increase both the amount and region of entanglement quantified by either the Meyer-Wallach measure or the concurrence. This is the case for both zero and finite temperatures. We have demonstrated that two quantum phase transitions exist in this system, signs of which are evident in both entanglement measures. In addition, we have calculated an entanglement witness that detects entanglement within a region which agrees with the measures of entanglement we consider.

It would be interesting to calculate the finite-temperature effects of the quantum phase transitions in this model. Determination of the effect on entanglement of increasing the period of the staggered parameters would also be an interesting extension to this work, for example, by variation of the magnetic field and coupling strength over three sites l, $l+1$, and $l+2$ rather than the two considered here. However, this may not be possible to do analytically.

ACKNOWLEDGMENTS

This work was supported by the Project for Developing Innovation Systems of the Ministry of Education, Culture, Sports, Science and Technology (MEXT), Japan. Y.N. acknowledges support from JSPS by KAKENHI (Grant No. 222812) and M.M. acknowledges support from JSPS by KAKENHI (Grant No. 23540463).

APPENDIX: CALCULATIONS OF QUANTITIES AT ZERO TEMPERATURE

Here, we give exact expressions of the ground-state energy, the magnetization at zero temperature, and the Meyer-Wallach measure of the ground state. For simplicity, we define regions such as

$$\mathcal{B}_1 := [0,\sqrt{J^2+b^2}), \tag{A1}$$

$$\mathcal{B}_2 := [\sqrt{J^2+b^2},\sqrt{j^2+b^2}), \tag{A2}$$

$$\mathcal{B}_3 := [\sqrt{j^2+b^2},\infty), \tag{A3}$$

$$\mathcal{B}_3' := [\sqrt{J^2+b^2},\infty). \tag{A4}$$

1. Ground-state energy

First, we show the exact expressions of the ground-state energy ϵ_g given by Eq. (15).

a. $j < J$

In this case, Q is given by

$$Q = (0,\Xi)\cup(\pi-\Xi,\pi). \tag{A5}$$

It is straightforward to calculate the ground-state energy

$$\epsilon_g = \begin{cases} \left(\frac{2}{\pi}\Xi - 1\right)B - \frac{2}{\pi}\int_0^{\Xi}\Theta(q)dq & \text{for} \quad B\in\mathcal{B}_1, \\ -B & \text{for} \quad B\in\mathcal{B}_3'. \end{cases} \tag{A6}$$

b. $j = J$

Since $\Lambda_q^- = 2B - 2\sqrt{J^2+b^2}$, the ground-state energy is obtained as

$$\epsilon_g = \begin{cases} -\sqrt{J^2+b^2} & \text{for} \quad B\in\mathcal{B}_1, \\ -B & \text{for} \quad B\in\mathcal{B}_3'. \end{cases} \tag{A7}$$

c. $j > J$

In this case, Q is given by

$$Q = (\Xi,\pi-\Xi). \tag{A8}$$

Then, the ground-state energy is calculated as

$$\epsilon_g = \begin{cases} -\frac{2}{\pi}\int_0^{\pi/2}\Theta(q)dq & \text{for} \quad B\in\mathcal{B}_1, \\ -\frac{2}{\pi}\Xi B - \frac{2}{\pi}\int_{\Xi}^{\pi/2}\Theta(q)dq & \text{for} \quad B\in\mathcal{B}_2, \\ -B & \text{for} \quad B\in\mathcal{B}_3. \end{cases} \tag{A9}$$

2. Magnetization at zero temperature

We show the magnetization at zero temperature per site m_g. The magnetization m_g is directly obtained from Eq. (7) as

$$m_g = \lim_{\beta\to\infty}\int_0^{\pi}\frac{dq}{2\pi}[\tanh(\beta\Lambda^+)+\tanh(\beta\Lambda^-)] = \int_{q\notin Q}\frac{dq}{\pi}. \tag{A10}$$

By substituting Q, the magnetization is obtained as follows: for $j < J$

$$m_g = \begin{cases} 1-\frac{2}{\pi}\Xi & \text{for} \quad B\in\mathcal{B}_1, \\ 1 & \text{for} \quad B\in\mathcal{B}_3'; \end{cases} \tag{A11}$$

for $j = J$,

$$m_g = \begin{cases} 0 & \text{for} \quad B\in\mathcal{B}_1, \\ 1 & \text{for} \quad B\in\mathcal{B}_3'; \end{cases} \tag{A12}$$

and, for $j > J$,

$$m_g = \begin{cases} 0 & \text{for} \quad B\in\mathcal{B}_1, \\ \frac{2}{\pi}\Xi & \text{for} \quad B\in\mathcal{B}_2, \\ 1 & \text{for} \quad B\in\mathcal{B}_3. \end{cases} \tag{A13}$$

3. Meyer-Wallach measure of the ground state

Here, we give the exact expressions for the Meyer-Wallach measure of the ground state, E_{MW}, given by Eq. (16). For $j < J$,

$$E_{\mathrm{MW}} = \begin{cases} \frac{4}{\pi}\Xi\left(1-\frac{\Xi}{\pi}\right) - \left(\frac{2b}{\pi}\int_0^{\Xi}\frac{1}{\Theta(q)}dq\right)^2 & \text{for} \quad B\in\mathcal{B}_1, \\ 0 & \text{for} \quad B\in\mathcal{B}_3'. \end{cases} \tag{A14}$$

For $j = J$,

$$E_{\mathrm{MW}} = \begin{cases} \frac{J^2}{J^2+b^2} & \text{for} \quad B\in\mathcal{B}_1, \\ 0 & \text{for} \quad B\in\mathcal{B}_3'. \end{cases} \tag{A15}$$

Finally, for $j > J$,

$$E_{\mathrm{MW}} = \begin{cases} 1 - \left(\frac{2b}{\pi}\int_0^{\pi/2} \frac{1}{\Theta(q)} dq\right)^2 & \text{for} \quad B \in \mathcal{B}_1, \\ 1 - \frac{4\Xi^2}{\pi^2} - \left(\frac{2b}{\pi}\int_{\Xi}^{\pi/2} \frac{1}{\Theta(q)} dq\right)^2 & \text{for} \quad B \in \mathcal{B}_2, \\ 0 & \text{for} \quad B \in \mathcal{B}_3. \end{cases} \tag{A16}$$

[1] L. Amico, R. Fazio, A. Osterloh, and V. Vedral, Rev. Mod. Phys. **80**, 517 (2008).
[2] D. P. DiVincenzo *et al*., Nature (London) **408**, 339 (2000).
[3] S. Bose, Phys. Rev. Lett. **91**, 207901 (2003).
[4] C. H. Bennett, H. J. Bernstein, S. Popescu, and B. Schumacher, Phys. Rev. A **53**, 2046 (1996).
[5] D. A. Meyer and N. R. Wallach, J. Math. Phys. **43**, 4273 (2002).
[6] K. M. O'Connor and W. K. Wootters, Phys. Rev. A **63**, 052302 (2001).
[7] G. Toth, Phys. Rev. A **71**, 010301(R) (2005).
[8] Č. Brukner and V. Vedral, e-print arXiv:quant-ph/0406040.
[9] S. Sachdev, *Quantum Phase Transitions* (Cambridge University Press, Cambridge, 1999).
[10] L. A. Wu, M. S. Sarandy, and D. A. Lidar, Phys. Rev. Lett. **93**, 250404 (2004).
[11] M. Oshikawa and I. Affleck, Phys. Rev. Lett. **79**, 2883 (1997).
[12] D. B. Abraham, J. Chem. Phys. **51**, 3795 (1969).
[13] P. Pincus, Solid State Commun. **9**, 1971 (1971).
[14] J. Hide, W. Son, I. Lawrie, and V. Vedral, Phys. Rev. A **76**, 022319 (2007).
[15] R. H. Crooks and D. V. Khveshchenko, Phys. Rev. A **77**, 062305 (2008).
[16] S. I. Doronin, A. N. Pyrkov, and E. B. Fel'dman, JETP **105**, 953 (2007).
[17] J. H. H. Perk, H. W. Capel, M. J. Zuilhof, and Th. J. Siskens, Physica A **81**, 319 (1975).
[18] E. Barouch and B. M. McCoy, Phys. Rev. A **3**, 786 (1971).
[19] J. H. H. Perk and H. W. Capel, Physica A **92**, 163 (1978).
[20] J. H. H. Perk, H. W. Capel, and Th. J. Siskens, Physica A **89**, 304 (1977).
[21] M. Takahashi, *Thermodynamics of One-Dimensional Solvable Models* (Cambridge University Press, Cambridge, 1999).
[22] G. K. Brennen, Quantum Inf. Comput. **3**, 619 (2003) [http://www.rintonpress.com/journals/qiconline.html].
[23] T. R. de Oliveira, G. Rigolin, and M. C. de Oliveira, Phys. Rev. A **73**, 010305(R) (2006).
[24] G. Rigolin, T. R. de Oliveira, and M. C. de Oliveira, Phys. Rev. A **74**, 022314 (2006).
[25] A. Montakhab and A. Asadian, Phys. Rev. A **82**, 062313 (2010).
[26] A. Osterloh, L. Amico, G. Falci, and R. Fazio, Nature (London) **416**, 608 (2002).
[27] T. R. de Oliveira, G. Rigolin, M. C. de Oliveira, and E. Miranda, Phys. Rev. Lett. **97**, 170401 (2006).
[28] T. R. de Oliveira, G. Rigolin, M. C. de Oliveira, and E. Miranda, Phys. Rev. A **77**, 032325 (2008).
[29] T. J. Osborne and M. A. Nielsen, Phys. Rev. A **66**, 032110 (2002).
[30] G. Muller and R. E. Shrock, Phys. Rev. B **32**, 5845 (1985).
[31] Y. Nakata, D. Markham, and M. Murao, Phys. Rev. A **79**, 042313 (2009).